Environ. Sci. Technol. **2008,** *42,* 1262–1267

Factors Affecting the Yield of Oxidants from the Reaction of Nanoparticulate Zero-Valent Iron and Oxygen

CHRISTINA R. KEENAN AND DAVID L. SEDLAK*

Department of Civil and Environmental Engineering University of California at Berkeley, Berkeley, California 94720

Received October 10, 2007. Revised manuscript received November 20, 2007. Accepted November 21, 2007.

The corrosion of zero-valent iron ($Fe^0_{(s)}$) by oxygen (O_2) can lead to the oxidation of organic compounds. To gain insight into the reaction mechanism and to assess the nature of the oxidant, the oxidation of methanol, ethanol, 2-propanol, and benzoic acid by the reaction of nanoparticulate zero-valent iron (nZVI) or ferrous iron (Fe[II]) with O_2 in the absence of ligands was studied. At pH values below 5, $Fe^0_{(s)}$ nanoparticles were oxidized by O_2 within 30 min with a stoichiometry of approximately two $Fe^0_{(s)}$ oxidized per O_2 consumed. The yield of methanol and ethanol oxidation products increased from 1% at acidic pH to 6% at pH 7, relative to nZVI added. Product yields from 2-propanol and benzoic acid were highest under acidic conditions, with little oxidation observed at neutral pH. At pH values below 5, product formation was attributable to hydroxyl radical (OH·) production through the Fenton reaction, involving hydrogen peroxide and Fe(II) produced during nZVI oxidation. At higher pH values, the oxidation of Fe(II), the initial product of nZVI oxidation, by oxygen is responsible for most of the oxidant production. Product yields at circumneutral pH values were consistent with a different oxidant, such as the ferryl ion (Fe[IV]).

Introduction

Zero-valent iron ($Fe^0_{(s)}$) is quickly oxidized to ferrous (Fe[II]) and ferric (Fe[III]) iron in the presence of oxygen. Although the reaction of $Fe^0_{(s)}$ with oxygen is undesirable in remedial applications that exploit the reductive capability of $Fe^0_{(s)}$ (*1*), it can lead to the formation of reactive oxygen species (ROS) capable of oxidizing contaminants that cannot be reduced by $Fe^0_{(s)}$. The $Fe^0_{(s)}$ and O_2 system can oxidize arsenic(III) (*2*) and several recalcitrant organic compounds, including 4-chlorophenol, pentachlorophenol, molinate, and EDTA (*3–6*). The production of oxidants by metal-containing nanoparticles is also an area of interest among toxicologists because ROS have been implicated in cell damage (*7*).

To explain oxidant production and reaction kinetics, two different reaction mechanisms have been proposed. In the first mechanism (Scheme 1), $Fe^0_{(s)}$ reacts with oxygen to produce hydrogen peroxide through a two-electron transfer (*4, 8*). In the second mechanism (Scheme 2), ferrous iron produced by $Fe^0_{(s)}$ oxidation reacts with oxygen through a series of one-electron transfers to produce hydrogen peroxide (*2, 3, 5, 6*). In both cases, H_2O_2 ultimately reacts with ferrous iron via the Fenton reaction to produce an oxidizing intermediate, which then reacts with the contaminant of interest. In either scheme, only a small fraction of the $Fe^0_{(s)}$ may be converted into oxidants because competing reactions can consume ROS.

The nature of the reaction products and overall yield may be affected by pH-dependent changes in the mechanism of the Fenton reaction. Although the hydroxyl radical (OH·) has often been considered as the species responsible for oxidation (e.g., 9), recent evidence suggests that an alternate oxidant, such as the ferryl ion (Fe[IV]), may be formed under some conditions. For example, previous studies have provided evidence for the production of an Fe(IV) species by the Fenton reaction (*10–13*), the Fenton reaction in the presence of EDTA (*14*), the photo-Fenton reaction (*15*), and by the oxidation of Fe(II) by oxygen at neutral pH values (*16, 17*). Fe(IV) is a weaker oxidant than OH· and is more selective than OH· in its reactions with organic compounds (*18*).

To establish the role of $Fe^0_{(s)}$ in oxidant production and to assess the relative importance of OH· and other oxidants, the oxidation of several probe compounds was studied during the oxidation of nanoparticulate zero-valent iron (nZVI) and ferrous iron by O_2 in pH-buffered systems. Methanol and ethanol were chosen as probes for oxidant generation because they do not interact with surfaces to an appreciable extent and their main oxidation products, formaldehyde and acetaldehyde, respectively, can be quantified at low concentrations. Benzoic acid and 2-propanol were chosen as probes because they are only oxidized by OH· and other strong oxidants.

Materials and Methods

Materials. All chemicals were reagent grade and were used as received except for 2,4-dinitrophenyl hydrazine (DNPH), which was recrystallized three times from acetonitrile. All solutions were prepared using 18 MΩ Milli-Q water from a Millipore system. Glassware was acid-washed and rinsed before use. The following buffers were used: sodium acetate (pH 4–5.5), 2-(N-morpholino)ethanesulfonic acid (MES; pH 6), piperazine-N,N′-bis(ethanesulfonic acid) (PIPES; pH 6.5–7.5), and sodium borate (pH 8–9). All buffer concentrations were 1 mM unless noted. Solutions at pH 3 were unbuffered. MES and PIPES were selected because they do not form complexes with Fe(II) or Fe(III) (*19*). The solution pH was adjusted when necessary using 1 N HNO_3 or 1 N NaOH. Nanoparticulate zero-valent iron was prepared daily as described previously (*20*). When this method is used, primary particles with a diameter between 1 and 100 nm and a surface area of 33.5 m^2/g are produced (*20*). Additional information on particles prepared by this method is available elsewhere (*21*). Ferrous iron stock solutions were prepared by dissolving ferrous sulfate in N_2-sparged 1 mM HNO_3.

Experimental Setup. All experiments were carried out at room temperature (20 ± 2 °C) in the dark in 60 mL glass serum vials. The vials were sealed with a rubber septa and had no headspace to prevent oxygen transfer to and from the solution. Although the concentration of oxygen decreased as iron was oxidized, the final O_2 concentration was never less than 80 μM. To initiate a reaction, an aliquot of nZVI and/or Fe(II) was added from a stock solution to air-saturated solutions containing 5–100 mM of the probe compound and 1–2 mM of buffer. The nZVI and/or Fe(II) concentration added was typically 150 μM ± 15 μM. The particles were kept in suspension by placing the reactors on an orbital shaker table at 150 rotations per minute. Samples were collected at

* Corresponding author phone: (510) 643-0256; fax: (510) 642-7483; e-mail: sedlak@ce.berkeley.edu.

10.1021/es7025664 CCC: $40.75
Published on Web 01/09/2008

SCHEME 1.

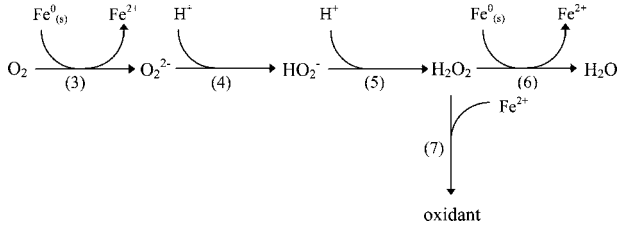

SCHEME 2.

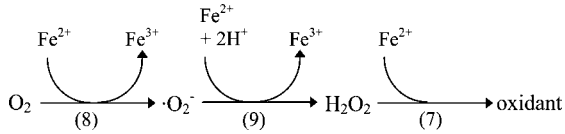

different time intervals using a 5 mL glass syringe and filtered immediately through a 0.22 μm nylon syringe filter (Fisher). The reactors were sacrificial, at least two reactors were sampled for each time point, and the data were averaged.

Analytical Techniques. A modified ferrozine method (*22*) was used to determine the concentration of dissolved Fe(II), total dissolved iron, and total iron. The method was further modified by adding an aliquot of ammonium fluoride (final concentration = 7 mM) before adding ferrozine to dissolved Fe(II) samples to prevent interference by Fe(III). Dissolved iron was defined as iron that passed through a 0.22 μm nylon syringe filter (Fisher). Total dissolved iron was quantified after adding hydroxylamine hydrochloride (final concentration = 60 mM) to filtered samples. Control experiments with freshly prepared nanoparticles indicated that nZVI did not pass through the filter (data not shown). Samples were analyzed on a UV–vis spectrophotometer at 562 nm (ϵ = 27900 M^{-1} cm^{-1}). All standard curves were linear with regression coefficients >0.9990, and the detection limit was 3 μM.

Because the nZVI stock was heterogeneous, it was difficult to ensure identical initial nZVI concentrations in each reactor. To address this issue, the total iron added in each experiment was quantified by acidifying the contents of the reactor at the end of the experiment and analyzing an unfiltered aliquot for total iron. Measured total iron concentrations agreed with the nominal concentration calculated from the concentration of the stock solution within 10%. Data were normalized by dividing by the total iron added to each reactor to allow for comparison of different data sets.

Dissolved oxygen was measured by colorimetric titration (*23*). The method was scaled down to use 5 mL of sample, but was otherwise unaltered. The detection limit was 15 μM.

Several probe compounds were used to quantify the production of reactive oxidants and study the nature of the oxidant. Use of relatively high concentrations of probe compounds assured that reactions between OH· and buffers or Fe[II] would not be important. Methanol is an appropriate compound because it has a low affinity for oxide surfaces and is neutral over the pH range of interest. The reaction of methanol with OH· is fast (Table 1) and only reactions 1 and 2 are important under the experimental conditions (i.e., [O_2] >> [Fe(III)]; *25, 27*):

$$OH\cdot + CH_3 \rightarrow \cdot CH_2OH + H_2O \quad (1)$$

$$\cdot CH_2OH + O_2 \rightarrow \cdot O_2CH_2OH \rightarrow + HCHO + H_2O\cdot \quad (2)$$

Relatively high concentrations of methanol (50–100 mM) were used to ensure that at least 98% of the OH· reaching the bulk solution reacted with the target compound (Table 1).

Three other probe compounds were used in this study. 2-propanol (50 mM) and benzoic acid (5–10 mM) were chosen because they are selective for OH·. Lower concentrations of benzoic acid (5–10 mM) were used due to limited solubility and the ability of benzoic acid to associate with surfaces at high concentrations. It is possible that MES or PIPES could have scavenged up to 20% of the OH·. However, this would not alter the trends or overall conclusion of these experiments. The maximum reported yield of acetone, the primary product from the reaction of 2-propanol and OH·, is 86.7% (85.5% by α abstraction and 1.2% by OH abstraction; 25). Benzoic acid reacts with OH· to form three isomers of hydroxybenzoic acid in the presence of oxygen. The isomers account for 90 ± 5% of the possible products, and the ortho, meta, and para isomers are reported to occur in the ratio 1.7:2.3:1.2 (*28*). Due to coelution of the ortho and meta forms and sensitivity issues, only para-hydroxybenzoic acid (p-HBA) was quantified.

Ethanol (50–100 mM) was also used as a probe because it is structurally similar to methanol and may react with both OH· and the ferryl ion (*18*). It reacts with OH·, and presumably Fe(IV), to form acetaldehyde. The reported maximum yield of acetaldehyde formation by the reaction of ethanol and OH· in the presence of O_2 is 86.8% (84.3% by α abstraction and 2.5% by OH abstraction (*25*)).

Formaldehyde (HCHO), acetaldehyde, and acetone, the oxidation products of methanol, ethanol, and 2-propanol, respectively, were determined using 2,4-dinitrophenylhydrazine (DNPH) derivatization followed by high-performance liquid chromatography (HPLC) and UV absorbance detection (*29, 30*). Benzoic acid and p-HBA concentrations were also determined by HPLC/UV. Detailed operating conditions are provided in the Supporting Information. All standard curves were linear with regression coefficients >0.9990, and the detection limits were <0.5 μM for the aldehydes, <1.6 μM for acetone, and <0.3 μM for p-HBA.

The reaction was quenched by filtering the nZVI from the solution through a 0.22-μm nylon syringe filter (Fisher). In some cases (e.g., first 15 min of pH 3 and 4 solutions), hydrogen peroxide was still present in solution and resulted in artificially high HCHO yields due to continuation of the Fenton reaction after filtration. In these cases, an aliquot of 1,10-phenanthroline (final concentration = 850 μM) was added to the filtered solutions to complex with ferrous iron and prevent the continuation of the Fenton reaction (*31*). Further oxidation of the product compounds by the reactive oxidant(s) was negligible because the product concentrations were low relative to the concentrations of the probe compounds.

Results

The introduction of nZVI to acidic methanol solutions produced a rapid burst of formaldehyde accompanied by the release of Fe(II) and the consumption of O_2 (Figure 1). After 30 min, dissolved Fe(II) accounted for 87 ± 1.7% of the added Fe and 94 ± 1% of the total dissolved iron. The ratio of O_2 consumed to initial nZVI was 0.51 ± 0.04 and the yield of HCHO produced per O_2 consumed was 1.1%

The release of dissolved iron and production of HCHO was slower at higher pH values, with continuous HCHO production for over 60 min at pH 5.5−8 (Figure 2). The maximum HCHO yield after completion of the reaction at 60 min was observed at near-neutral pH (Figure 3). At pH values above 4, less iron passed through the filter due to increased Fe(II) and Fe(III) precipitation or adsorption on the nZVI particles (72 ± 5% at pH 5, 47 ± 9% at pH 6). The precipitates at pH values above 5 were qualitatively very different than the parent nZVI particles in appearance (e.g., rusty rather than black and more uniform in appearance). This is consistent with previous observations that the

TABLE 1. Selected Published Rate Constants for Reactions of OH·

compound	reaction	k (M^{-1} s^{-1})	reference
acetate	$CH_3CO_2^- + OH\cdot \rightarrow \cdot CH_2CO_2^- + H_2O$	8.5×10^7	*24*
acetic acid	$CH_3CO_2H + OH\cdot \rightarrow \cdot CH_2CO_2H + H_2O$	1.6×10^7	*24*
benzoate	$C_6H_5CO_2^- + OH\cdot \rightarrow HOC_6H_4CO_2H$	4.3×10^9	*24*
benzoic acid	$C_6H_5CO_2H + OH\cdot \rightarrow HOC_6H_5CO_2H$	5.9×10^9	*24*
borate	$B(OH)_4^- + OH\cdot \rightarrow$	$<1 \times 10^6$	*24*
ethanol	$CH_2H_5OH + OH\cdot \rightarrow CH_3\cdot CHOH$ (84.3%) + $CH_3CH_2O\cdot$ (2.5%) + $\cdot CH_2CH_2OH$ (13.2%) + H_2O	1.9×10^9	*24,25*
Fe(II)	$Fe(II) + OH\cdot \rightarrow Fe(III) + OH^-$	5.0×10^8	*26*
methanol	$CH_3OH + OH\cdot \rightarrow \cdot CH_2OH + H_2O$	9.7×10^8	*24*
2-propanol	$(CH_3)_2CHOH + OH\cdot \rightarrow (CH_3)_2\cdot COH$ (85.5%) + $(CH_3)_2CHO\cdot$ (1.2%) + $\cdot CH_2CHOHCH_3$ (13.3%) + H_2O	1.9×10^9	*24,25*

products of nZVI oxidation are formed by oxidative dissolution followed by precipitation (*21*).

Experiments were performed with ferrous iron added to the methanol solution, rather than nZVI, to assess the role of Fe(II) in oxidant production (Scheme 2; dotted lines in Figure 3). Significant HCHO production was only observed at pH values above 6 because homogeneous Fe(II) oxidation by O_2 is strongly pH dependent with half-lives greater than 450 h at pH values less than 5.5 under these conditions (*32*). Under acidic conditions, nearly all of the Fe(II) added was recovered in its initial unreacted form after filtration (inset of Figure 3).

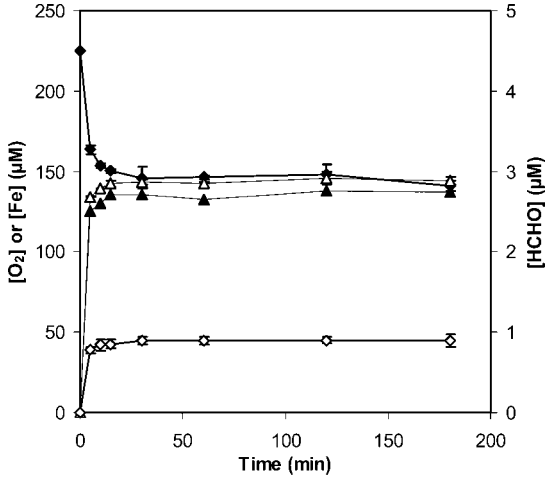

FIGURE 1. Concentration of dissolved oxygen (♦), HCHO (◊), dissolved ferrous (▲) and total iron (Δ). Initial conditions: 150 μM ± 15 μM nZVI added to air-saturated 100 mM CH_3OH. Initial pH 2.9, final pH 3.3.

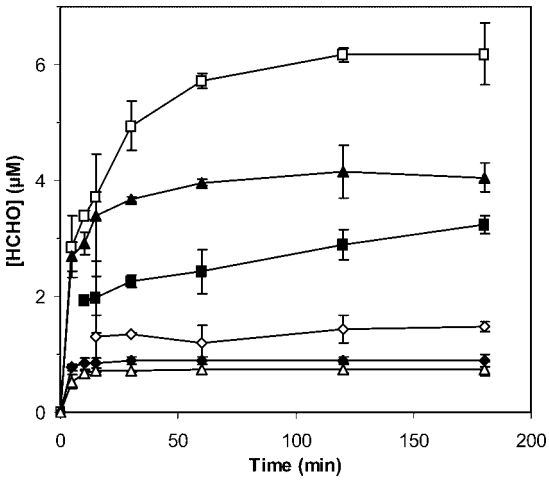

FIGURE 2. HCHO generation over time. Reaction conditions: 150 ± 15 μM nZVI added to air-saturated 100 mM CH_3OH and 1 mM buffer as described in the text. Initial pH: 3.1 (♦), 4.4 (◊), 5.5 (■), 7 (□), 8 (▲), 9 (Δ).

It is possible that the presence of the oxide coating of the nZVI particles accelerated the oxidation of ferrous iron by oxygen at lower pH values (*33*). To assess this phenomenon, aliquots of ferrous iron were added to solutions containing 100 mM CH_3OH and 150 μM nZVI ± 20 μM at pH 5, 6, and 7 (Figure 4). Increases in HCHO production with Fe(II) addition were higher at pH 7 than at pH 5 and 6.

Ethanol, benzoic acid, and 2-propanol also were used as probe compounds to assess the nature of the oxidant produced in the nZVI and oxygen system (Figure 5). The yield of acetaldehyde, the oxidation product of ethanol, followed the same trends as the yield of formaldehyde with the highest yields observed at neutral pH. Acetaldehyde yields were 65 ± 7% of the HCHO yields at all pH values. The yields of para-hydroxybenzoic acid and acetone, the oxidation products of benzoic acid and 2-propanol, respectively, followed a very different trend. The maximum yields were observed at pH 3 (the lowest pH studied) and product yield decreased as pH increased. At pH 3, the p-HBA and acetone yields were 2.4 and 11.9 times higher than the HCHO yields, respectively. In Fenton control experiments (pH 3, 150 μM Fe(II) and 25 μM H_2O_2; Supporting Information (SI) Figure 1),

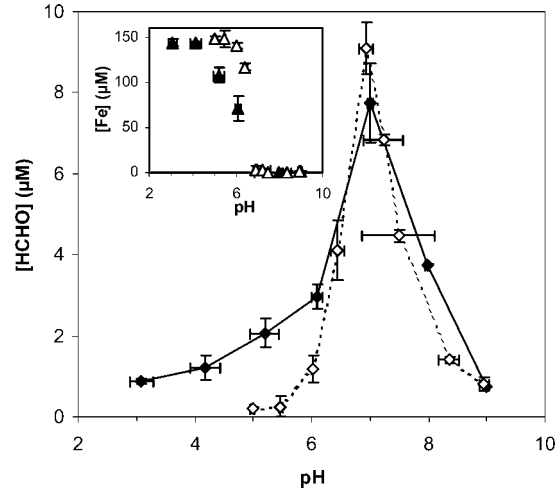

FIGURE 3. pH dependence of HCHO production and dissolved iron generation (inset) at 60 min. Reaction conditions: 150 μM ± 15 μM nZVI (solid points) or ferrous iron (hollow points) added to air-saturated 100 mM CH_3OH and 1–2 mM buffer as described in the text. The error bars on the *x*-axis represent the change in pH during each experiment; the error bars on the *y*-axis are the standard deviation of all data collected at each pH.

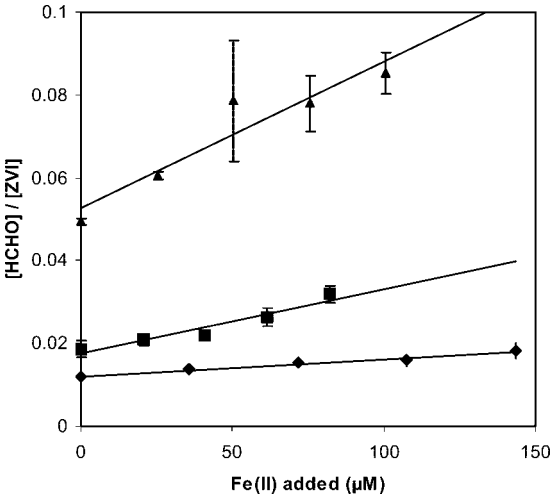

FIGURE 4. HCHO production normalized by nZVI added. Varied amounts of Fe(II) added to 150 μM ± 15 μM nZVI in 100 mM CH_3OH and 2 mM buffer. Initial pH: 5 (♦), 6 (■), 7 (▲).

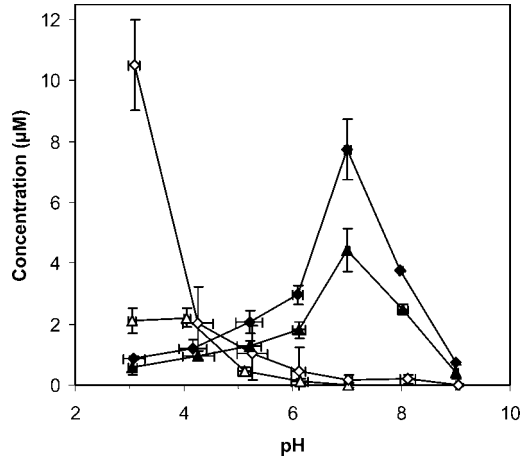

FIGURE 5. HCHO, acetaldehyde, pHBA and acetone production at 60 min as a function of pH. Reaction conditions: 150 μM ± 15 μM nZVI added to air-saturated 100 mM CH_3OH (♦), 100 mM ethanol (▲), 50 mM 2-propanol (◊), or 5 mM benzoic acid (Δ) and 1–2 mM buffer as described in text.

the yields of p-HBA and acetone were 1.4 and 11.3 times higher than the yields of HCHO.

Discussion

Reaction Mechanism. Mechanistic studies of iron corrosion indicate that oxygen is reduced via a series of two-electron transfers on the iron surface and in the bulk solution (reactions 3–6; *34, 35*). It is possible that a small fraction of the H_2O_2 reacts with ferrous iron via the Fenton reaction to produce a reactive oxidant instead of with $Fe^0_{(s)}$ (reaction 7).

The overall stoichiometry of reactions 3−6 is 0.5 mol O_2 reduced for every $Fe^0_{(s)}$ oxidized and is consistent with experiments conducted under acidic conditions (Figure 1). If 1.1% of oxygen goes through the two-electron transfer pathway (e.g., via reaction 7; equivalent to HCHO yield in Figure 1), the ratio of O_2 to $Fe^0_{(s)}$ would be 0.508:1, a slight difference that is within the error of the oxygen and $Fe^0_{(s)}$ measurements. Iron began precipitating above pH 4 (inset of Figure 3), making it difficult to close the oxygen and iron mass balances.

In Scheme 1 (reactions 3−7), the relative rates of reactions 6 and 7 control the yield of OH•. H_2O_2 reacts with $Fe^0_{(s)}$ (reaction 6) at rates that are approximately 2 orders of magnitude faster than with Fe(II) (reaction 7) based on HCHO yields of 1.1% (Figure 1). The rapid generation of HCHO is consistent with rapid production of H_2O_2 followed by the Fenton reaction. Under the conditions in Figure 1, the half-life of H_2O_2 produced during the first minute of nZVI oxidation would be approximately 90 s (*20, 31*).

The oxidation of Fe(II) by oxygen may also produce H_2O_2 (reactions 8–9; *32, 36, 37*). This reaction is then followed by the Fenton reaction (reaction 7) to produce a reactive oxidant, which is responsible for the oxidation of the probe compound. Assuming an air-saturated solution with a dissolved oxygen concentration of 250 μM, the half-life of reaction 8 is approximately 45 h at pH 6, 4.5 h at pH 6.5, and 27 min at pH 7 (*38*).

Due to the slow oxidation of Fe(II) by oxygen (reaction 8), oxidant production via Scheme 2 should be negligible in a homogeneous solution below pH 6.5 at the time-scales of interest in this study. However, it is possible that the presence of surfaces may accelerate the reaction at lower pH values (*33*). The slopes of the curves in Figure 4 suggest that surface-catalyzed Fe(II) oxidation was important to probe oxidation in these experiments at pH values above 6. The slope of the pH 5 data is not statistically different from zero ($p < 0.005$), indicating that $Fe^0_{(s)}$ alone is responsible for HCHO generation. The slope was significant at pH 6, suggesting that the surface-catalyzed ferrous iron oxidation contributes to probe oxidation. The slope of the pH 7 data is twice that of the pH 6 data, demonstrating that more Fe(II) oxidation occurs as pH increases as expected based on bulk phase Fe(II) oxidation rates (*32*). In the homogeneous system at pH 6, the oxidation of ferrous iron produced about 40% of the HCHO produced by similar concentrations of $Fe^0_{(s)}$ after 60 min (Figure 3). The presence of dissolved ferrous iron after nZVI oxidation under acidic conditions and its absence at pH values above 6 (inset of Figure 3) is consistent with the transition from Scheme 1 under acidic conditions to Scheme 2 at neutral pH values.

Above pH 7, the production of reactive oxidants can be attributed mainly to the reaction of ferrous iron with oxygen (Scheme 2). This conclusion is supported by the nearly identical formaldehyde yields when $Fe^0_{(s)}$ or Fe(II) alone were added to the reactors at the same concentrations (Figure 3). nZVI contributes to oxidant generation by serving as a source of Fe(II) and the contribution from Scheme 1 is negligible. This agrees well with the conclusions of Leupin and Hug (*2*) in a study of arsenic oxidation by $Fe^0_{(s)}$.

The yield of HCHO decreases above pH 7 (Figures 2 and 3). One possible explanation for the decreased yield is a change in reaction mechanism when Fe(II) is associated with a mineral or a surface. Ferrous hydroxide ($Fe(OH)_{2(s)}$) is the least soluble Fe(II) species in the absence of bicarbonate. Using a solubility product of 3×10^{-16} (*39*), a solution of 150 μM Fe(II) (the typical amount of Fe used in this study) will be oversaturated at pH 8.15. It is likely that the affinity of Fe^{2+} for the surface of a $Fe^0_{(s)}$ particle or a ferric oxide coated surface also would increase with pH. Ferric iron has limited solubility above neutral pH (*40*) and its rapid precipitation could also help explain the reduction in yield at high pH values.

Reactive Oxidant Production. In both proposed reaction mechanisms, the Fenton reaction is ultimately responsible for the production of the reactive oxidant. Although the oxidizing capability of the Fenton reaction was established over 100 years ago (*41*), the identity of the oxidant produced by the reaction is still unresolved. The hydroxyl radical has often been cited as the main oxidant (reaction 7; *9, 42*). However, thermodynamic considerations suggest that the reaction occurs via an inner-sphere water exchange mech-

anism rather than an outer-sphere mechanism as indicated in reaction 7 (*43*):

$$[Fe(OH)(H_2O)_5]^+ + H_2O_2 \rightarrow [Fe(OH)(H_2O_2)(H_2O)_4]^+ + H_2O \quad (10)$$

The iron-peroxide complex may dissociate to form OH· or a ferryl (Fe[IV]) species (*43*):

$$[Fe(OH)(H_2O_2)(H_2O)_4]^+ \rightarrow [Fe(OH)(H_2O)_4]^{2+} + OH^{\cdot} + OH^- \quad (11)$$

$$[Fe(OH)(H_2O_2)(H_2O)_4]^+ \rightarrow [Fe(OH)(H_2O)_4]^{3+} + 2OH^- \quad (12)$$

The ferryl ion species formed in reaction 12 may also react with water to form OH· (e.g., 10). Solution conditions, such as pH and the presence of ligands (e.g., EDTA), play an important role in determining the relative rates of reactions 11 and 12. For example, Hug and Leupin (*11*) concluded that the Fenton reaction produced OH· at low pH and a different oxidant, most likely an Fe(IV) species, at higher pH based on the inability of 2-propanol to quench the reaction. Pignatello et al. (*15*) found that the photo-Fenton system (Fe^{3+}/H_2O_2/UV) produced a mixture of OH· and ferryl ion at pH 2.8, whereas the standard Fenton system produced exclusively OH· under acidic conditions. Rush and Koppenol (*14*) found that the Fe^{II}EDTA complex formed an intermediate other than OH· at pH 7.3.

OH· is a nonselective oxidant and reacts at near-diffusion controlled rates with many organic compounds (Table 1). However, the ferryl ion is less reactive than OH· and has a longer lifetime in solution in the absence of H_2O_2 (*10*). However, few rate constants are available for Fe(IV) reactions with organic compounds. Jacobsen et al. (*18*) reported much higher reactivity of the ferryl ion (FeO^{2+}) with ethanol ($k = 2.5 \times 10^3\ M^{-1}\ s^{-1}$) than benzoic acid ($k = 8.0 \times 10^1\ M^{-1}\ s^{-1}$). This difference in rate constants corresponds well with observations that the ferryl intermediate in the Fenton reaction could be scavenged significantly better by ethanol than by benzoate (*14*).

The probe compounds used in this study provide insight into the nature of oxidant(s) produced when $Fe^0_{(s)}$ reacts with O_2. The primary alcohols, methanol and ethanol, were oxidized over a wide pH range, whereas benzoic acid and 2-propanol oxidation were only detected below pH 7 and was highest at pH 3 (Figure 5). The ability of the $Fe^0_{(s)}$ and oxygen system to oxidize all four probe compounds under acidic conditions is consistent with OH· production by reaction 7 (Scheme 1). The decrease in benzoate and 2-propanol oxidation as pH increased from 3 to 7 suggests that less OH· is produced. However, the increased yield of methanol and ethanol oxidation products up until pH 7 suggests the production of an alternate oxidant, such as the ferryl ion.

Each probe compound produced different yields at pH 3 (Figure 5), even though equivalent yields were expected based on rate constants with OH· (Table 1). Similar ratios of products were found in Fenton control experiments (SI Figure S1), suggesting that the different yields are not due to the presence of $Fe^0_{(s)}$ surfaces. The difference in yields may be related to the reactions of intermediates produced after the initial reaction with OH·. HCHO yields at neutral pH were less than the maximum theoretical yields of 33% based in Scheme 2. This could be due to competing reactions of the oxidant with other species (e.g., with Fe[III]) or loss of ferrous iron due to coprecipitation with Fe(III). These discrepancies warrant further study.

Implications for Contaminant Oxidation and Toxicity. The nanoparticulate zero-valent iron and oxygen system may be useful for remediation under certain conditions. $Fe^0_{(s)}$ may serve as a source of OH· at acidic pH values in ex situ treatment systems. A similar approach has been suggested for remediation of pesticide-contaminated waste using $Fe^0_{(s)}$ electrodes as the source of $Fe^0_{(s)}$ (*44*). In the circumneutral pH range, $Fe^0_{(s)}$ and oxygen may serve as a source of a more selective oxidant (most likely Fe[IV]). While this remediation approach will only be applicable to contaminants that react quickly with Fe(IV), the selectivity may offer an advantage in the presence of OH· scavengers, such as bicarbonate and natural organic matter (NOM). In the absence of ligands (e.g., EDTA), arsenite appears to be an ideal candidate for oxidation by $Fe^0_{(s)}$ and oxygen (*2*). Future research is needed to improve oxidant yield by the addition of ligands and to identify other contaminants than can be degraded by the reactive species.

These results also have interesting implications for the potential toxicity of nanoparticles (e.g., ref *7*). Although iron is an essential element for growth of nearly all species, an abundance of free or loosely chelated iron has been linked to DNA damage, lipid peroxidation, and oxidative protein damage in vivo (*45*). Exposure (i.e., by inhalation) to $Fe^0_{(s)}$ nanoparticles may result in a release of Fe(II), followed by oxidative damage due to Fe(IV) generation.

Acknowledgments

This research was funded by the U.S. National Institute for Environmental Health Sciences (NIEHS) Superfund Basic Research Program (E5004705). We thank David Waite and Changha Lee for their advice and support.

Supporting Information Available

Detailed HPLC operating conditions and a figure containing pH 3 Fenton control results. This material is available free of charge via the Internet at http://pubs.acs.org.

Literature Cited

(1) Mackenzie, P. D.; Horney, D. P.; Sivavec, T. M. Mineral precipitation and porosity losses in granular iron columns. *J. Hazard. Materials* **1999**, *68*, 1–17.
(2) Leupin, O. X.; Hug, S. J. Oxidation and removal of arsenic(III) from aerated groundwater by filtration through sand and zero-valent iron. *Water Res.* **2005**, *39*, 1729–1740.
(3) Noradoun, C.; Engelmann, M. D.; McLaughlin, M.; Hutcheson, R.; Breen, K.; Paszczynski, A.; Cheng, I. F. Destruction of chlorinated phenols by dioxygen activation under aqueous room temperature and pressure conditions. *Ind. Eng. Chem. Res.* **2003**, *42*, 5024–5030.
(4) Joo, S. H.; Feitz, A. J.; Waite, T. D. Oxidative degradation of the carbothioate herbicide, molinate, using nanoscale zero-valent iron. *Environ. Sci. Technol.* **2004**, *38*, 2242–2247.
(5) Noradoun, C. E.; Cheng, I. F. EDTA degradation induced by oxygen activation in a zero-valent iron/air/water system. *Environ. Sci. Technol.* **2005**, *39*, 7158–7163.
(6) Englehardt, J. D.; Meeroff, D. E.; Echegoyen, L.; Deng, Y.; Raymo, F. M.; Shibata, T. Oxidation of aqueous EDTA and associated organics and coprecipitation of inorganics by ambient iron-mediated aeration. *Environ. Sci. Technol.* **2007**, *41*, 270–276.
(7) Nel, A.; Xia, T.; Mädler, L.; Li, N. Toxic potential of materials at the nanolevel. *Science* **2006**, *311*, 622–627.
(8) Joo, S. H.; Feitz, A. J.; Sedlak, D. L.; Waite, T. D. Quantification of the oxidizing capacity of nanoparticulate zero-valent iron. *Environ. Sci. Technol.* **2005**, *39*, 1263–1268.
(9) Walling, C. Fenton's reagent revisited. *Acc. Chem. Res.* **1975**, *8*, 125–131.
(10) Bossmann, S. H.; Oliveros, E.; Göb, S.; Siegwart, S.; Dahlen, E. P.; Payawan, L.; Straub, M.; Wörner, M.; Braun, A. M. New evidence against hydroxyl radicals as reactive intermediates in the thermal and photochemically enhanced Fenton reactions. *J. Phys. Chem. A.* **1998**, *102*, 5542–5550.
(11) Hug, S. J.; Leupin, O. Iron-catalyzed oxidation of arsenic(III) by oxygen and by hydrogen peroxide: pH-dependent formation of oxidants in the Fenton reaction. *Environ. Sci. Technol.* **2003**, *37*, 2734–2742.
(12) Kremer, M. L. Mechanism of the Fenton reaction: Evidence for a new intermediate. *Phys. Chem. Chem. Phys.* **1999**, *1*, 3595–3605.

(13) Wink, D. A.; Nims, R. W.; Desrosiers, M. F.; Ford, P. C.; Keefer, L. K. A kinetic investigation of intermediates formed during the Fenton reagent mediated degradation of *N*-nitrosodimethlamine: Evidence for an oxidative pathway not involving hydroxyl radical. *Chem. Res. Toxicol.* **1991**, *4*, 510–512.
(14) Rush, J. D.; Koppenol, W. H. Oxidizing intermediates in the reaction of ferrous EDTA with hydrogen peroxide: Reactions with organic molecules and ferrocytochrome-c. *J. Bio. Chem.* **1986**, *261*, 6730–6733.
(15) Pignatello, J. J.; Liu, D.; Huston, P. Evidence for an additional oxidant in the photoassisted Fenton reaction. *Environ. Sci. Technol.* **1999**, *33*, 1832–1839.
(16) Hug, S. J.; Canonica, L.; Wegelin, M.; Gecther, D.; Von Gunten, U. Solar oxidation and removal of arsenic at circumneutral pH in iron containing waters. *Environ. Sci. Technol.* **2001**, *35*, 2114–2121.
(17) Reinke, L. A.; Rau, J. M.; McCay, P. B. Characteristics of an oxidant formed during iron(II) autoxidation. *Free Radical Biol. Med.* **1994**, *16*, 485–492.
(18) Jacobsen, F.; Holcman, J.; Sehested, K. Reactions of the ferryl ion with some compounds found in cloud water. *Int. J. Chem. Kinet.* **1998**, *30*, 215–221.
(19) Yu, Q. Y.; Kandegedara, A.; Xu, Y. P.; Rorabacher, D. B. Avoiding interferences from Good's buffers: A contiguous series of noncomplexing tertiary amine buffers covering the entire range of pH 3–11. *Anal. Biochem.* **1997**, *253*, 50–56.
(20) Wang, C. B.; Zhang, W. X. Synthesizing nanoscale iron particles for rapid and complete dechlorination of TCE and PCBs. *Environ. Sci. Technol.* **1997**, *31*, 2154–2156.
(21) Nurmi, J. T.; Tratnyek, P. G.; Sarathy, V.; Baer, D. R.; Amonette, J. E.; Pecher, K.; Wang, C.; Linehan, J. C.; Matson, D. W.; Penn, R. L.; Driessen, M. D. Characterization and properties of metallic iron nanoparticles: Spectroscopy, electrochemistry, and kinetics. *Environ. Sci. Tecnhol.* **2005**, *39*, 1221–1230.
(22) Voelker, B. M.; Sulzberger, B. Effects of fulvic acid on Fe(II) oxidation by hydrogen peroxide. *Environ. Sci. Technol.* **1996**, *30*, 1106–1114.
(23) *Standard Methods for the Examination of Water and Wastewater*, 18th ed.; APHA, AWWA, and WEF: Washington, DC, 1992; pp 4–98–4–102.
(24) Buxton, G. V.; Greenstock, C. L.; Helman, W. P; Ross, A. B. Critical review of rate constants for reactions of hydrated electrons, hydrogen atoms and hydroxyl radicals in aqueous solutions. *J. Phys. Chem. Ref. Data.* **1988**, *17*, 513–886.
(25) Asmus, K. D.; Möckel, H.; Henglein, A. Pulse radiolytic study of the site of OH· radical attach on aliphatic alcohols in aqueous solution. *J. Phys. Chem.* **1973**, *77*, 1218–1221.
(26) Farhataziz; Ross, A. B. *Selected Specific Rates of Reactions of Transients from Water in Aqueous Solution, III, Hydroxyl Radical and Perhydroxyl Radical and Their Radical Ions*; Report NSRDS-NBS 59; Washington, D. C., 1977.
(27) Hess, W. P.; Tully, F. P. Hydrogen-atom abstraction from methanol by OH. *J. Phys. Chem.* **1989**, *93*, 1944–1947.
(28) Klein, G. W.; Bhatia, K.; Madhavan, V.; Schuler, R. H. Reaction of ·OH with benzoic acid: Isomer distribution in the radical intermediates. *J. Phys. Chem.* **1975**, *79*, 1767–1774.
(29) Zhou, X. L.; Mopper, K. Determination of photochemically produced hydroxyl radicals in seawater and freshwater. *Mar. Chem.* **1990**, *30*, 71–88.
(30) Grannas, A. M.; Martin, C. B.; Chin, Y. P.; Platz, M. Hydroxyl radical production from irradiated Arctic dissolved organic matter. *Biogeochemistry* **2006**, *78*, 51–66.
(31) Duesterberg, C. K.; Cooper, W. J.; Waite, T. D. Fenton-mediated oxidation in the presence and absence of oxygen. *Environ. Sci. Technol.* **2005**, *39*, 5052–5058.
(32) Singer, P. L.; Stumm, W. Acidic mine drainage: The rate-determining step. *Science* **1970**, *167*, 1121–1123.
(33) Tamura, H.; Goto, K.; Nagayama, M. The effect of ferric hydroxide on the oxygenation of ferrous ions in neutral solutions. *Corros. Sci.* **1976**, *16*, 197–207.
(34) Zecevic, S.; Drazic, D. M.; Gojkovic, S. Oxygen reduction on iron. Part III. An analysis of the rotating disk-ring electrode measurements in near neutral solutions. *J. Electroanal. Chem.* **1989**, *265*, 179–193.
(35) Zecevic, S.; Drazic, D. M.; Gojkovic, S. Oxygen reduction on iron. Part IV. The reduction of hydrogen peroxide as the intermediate in oxygen reduction reaction in alkaline solutions. *Electrochim. Acta* **1991**, *36*, 5–14.
(36) Stumm, W.; Lee, G. F. Oxygenation of ferrous iron. *Ind. Eng. Chem.* **1961**, *53*, 143–146.
(37) Millero, F. J.; Izaguirre, M. Effect of ionic strength and ionic interactions on the oxidation of Fe(II). *J. Solution Chem.* **1989**, *18*, 585–599.
(38) King, D. W.; Lounsbury, H. A.; Millero, F. J. Rates and mechanism of Fe(II) oxidation at nanomolar total iron concentrations. *Environ. Sci. Technol.* **1995**, *29*, 818–824.
(39) Leussing, D. L.; Kolthoff, I. M. The solubility product of ferrous hydroxide and the ionization of the aquo-ferrous ion. *J. Am. Chem. Soc.* **1953**, *75*, 2476–2479.
(40) Baes C. F.; Mesmer R. E. *The Hydrolysis of Cations*; John Wiley & Sons, Inc.: New York, 1975; pp 226–237.
(41) Fenton, H. J. H. Oxidation of tartaric acid in the presence of iron. *J. Chem. Soc.* **1894**, *65*, 899–910.
(42) Haber, F.; Weiss, J. On the catalysis of hydroperoxide. *Naturwissenschaften* **1932**, *20*, 948–950.
(43) Goldstein, S.; Meyerstein, D.; Czapski, G. The Fenton reagents. *Free Radical Biol. Med.* **1993**, *15*, 435–445.
(44) Zhang, H. C.; Lemley, A. T. Reaction mechanism and kinetic modeling of DEET degradation by flow-through anodic Fenton treatment (FAFT). *Environ. Sci. Technol.* **2006**, *40*, 4488–4494.
(45) Valko, M.; Morris, H.; Cronin, M. T. D. Metals, toxicity and oxidative stress. *Curr. Med. Chem.* **2005**, *12*, 1161–1208.

ES7025664